JOURNAL OF GEOPHYSICAL RESEARCH, VOL. 101, NO. B7, PAGES 16,101–16,118, JULY 10, 1996

Slip in the 1868 Hayward earthquake from the analysis of historical triangulation data

Ellen Yu and Paul Segall

Department of Geophysics, Stanford University, Stanford, California

Abstract. Despite the importance of the Hayward fault for earthquake hazards in the San Francisco Bay area, neither the rupture length nor the average coseismic slip in the most recent major earthquake, which occurred in 1868, is well known. We estimate slip in the 1868 earthquake by analyzing triangulation data collected between 1853-1860 and 1876-1891. We apply a denuisancing procedure that projects out the dependence of that data on station coordinates, allowing their displacements to be estimated directly. The best fit to the data is obtained with a 52-km-long by 10-km-deep rupture that extends from Warm Springs to near Berkeley, considerably longer than the 30 km of reported surface breakage. The estimated slip for an earthquake of this length is 1.9 ± 0.4 m, and the seismic moment is $M_0 = 3.0\ (\pm 0.7) \times 10^{19}$ N m, corresponding to M_w 7.0. The data are inconsistent with regionally high strain rate prior to the 1906 earthquake, as had been previously suggested. The triangulation data record northeastward displacement of station Loma Prieta, presumably as a result of the 1865 earthquake. The fault normal displacement is not easily explained by slip on either the San Andreas fault or the 1989 Loma Prieta rupture surface. This observation is, however, consistent with a $M_W \sim 6$ 3/4 thrust event northeast of the San Andreas fault in the southern Santa Cruz mountains thrust belt.

Introduction

The most recent large earthquake on the Hayward fault, which runs through the heavily populated east San Francisco Bay area, occurred on October 21, 1868. The combination of its location, history of large earthquakes, and elapsed time since the last major event makes the Hayward fault one of the most hazardous faults in California. As the 1868 quake occurred before the advent of instrumental seismology, very little is known quantitatively about the event. The magnitude is estimated to have been M 7.2 based on comparison of the 1868 isoseismals with those of the 1984 Morgan Hill and 1989 Loma Prieta earthquakes [*Toppozada et al.,* 1992]. In 1987 the California Division of Mines and Geology estimated that a M 7.5 event on the Hayward fault would result in 1000 to 4000 fatalities, 4000 to 13,000 hospitalizations, and economic losses of tens of billions of dollars [*California Department of Conservation, Division of Mines and Geology,* 1987]. In light of the 1994 Northridge and 1995 Kobe earthquakes, it seems likely that economic losses could be far larger. Despite the importance of the 1868 earthquake for earthquake hazards in the San Francisco Bay area, neither the rupture length nor the average slip in the 1868 earthquake is well known.

Paper number 96JB00806.
0148-0227/96/96JB-00806$09.00

We do know that the 1868 earthquake ruptured the ground surface for at least 30 km of the Hayward fault from Warm Springs, at its southeastern end, northwest to San Leandro [*Lawson,* 1908] (heavy line in Figure 1). The surface break may have extended past San Leandro to the vicinity of Mills College (east of Oakland) (dashed line in Figure 1), however reports were incomplete, as the data were limited to "reports of cow-boys riding the range" [*Lawson,* 1908, p.434]. *Lienkaemper and Borchardt* [1992] suggest that the 1868 rupture may have terminated at a salient in the fault trace near Oakland and give an upper bound on rupture length of 41 km. On the other hand, *Toppozada et al.* [1981] show that intensities were uniformly high (Modified Mercalli Intensity VIII) for $\sim$ 50 km along the fault, from Warm Springs northwest to Berkeley.

Measurements of surface displacement also exist for the 1868 event, but they are often ambiguous about the sense of displacement or even as to whether the measurement was of fault offset. Right-lateral offsets of 0.10 to 0.15 m were measured in Hayward [*Lawson,* 1908]; however, these are anomalously small for a M 7 earthquake. Surface slip often significantly underestimates slip at depth [*Thatcher and Lisowski,* 1987], particularly on faults that exhibit shallow fault creep, such as the Hayward. Displacements of 0.9 m reported by *Lawson* [1908] are widely cited, but as *Lienkaemper and Borchardt* [1992, p.104] noted, Lawson "refers to vertical and extensional components in this discussion with no mention of strike-slip."

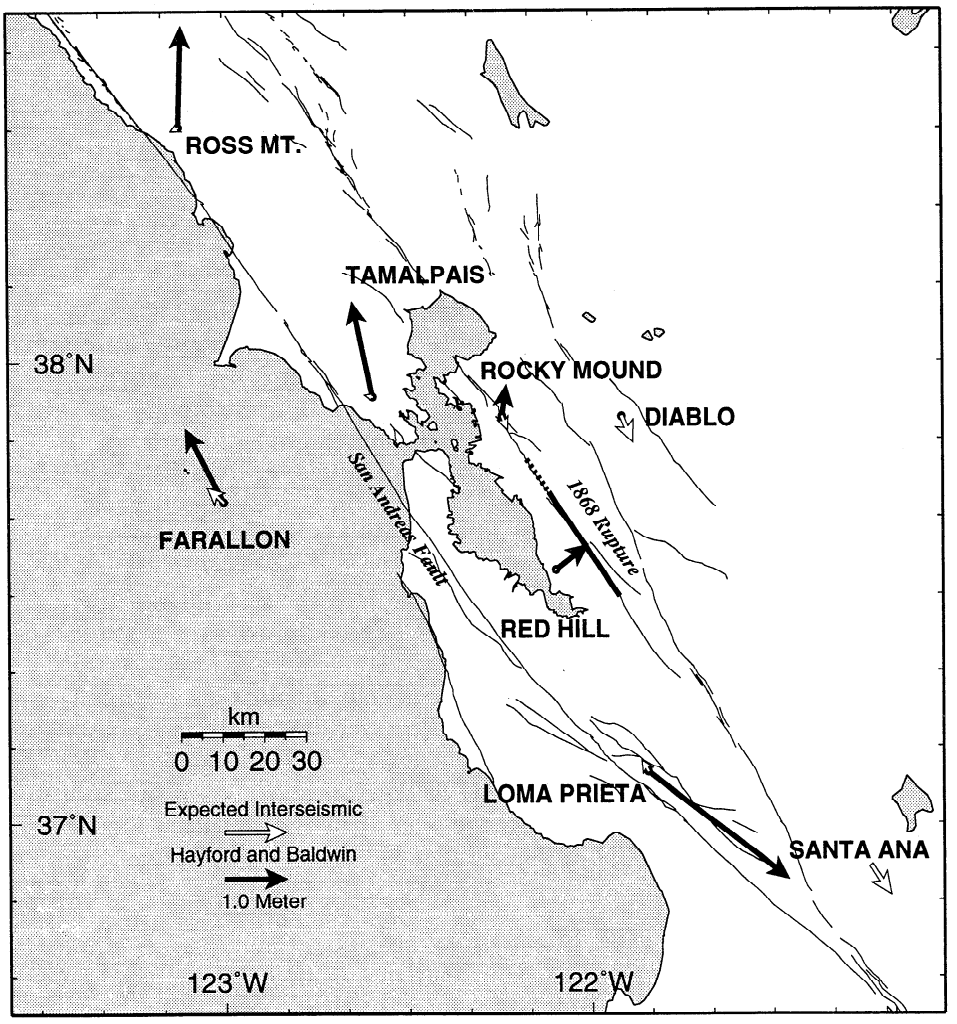

Figure 1. Displacements for the period 1851-1891 computed by *Hayford and Baldwin* [1908] (solid arrows), which they attributed to the 1868 earthquake. Diablo was held fixed, and other (not well documented) assumptions were made to determine the change in direction and length between Diablo and Tamalpais. The 1868 rupture is shown by the solid line for 30 km northwest of Warm Springs and dashed for an additional 10 km. The expected interseismic displacements for the 30 year interval 1855-1885 are shown for comparison (open arrows).

Little is known about previous earthquakes on the Hayward Fault. In the absence of historic or geologic records of past earthquakes, hazard assessments are often based on a "time predictable" recurrence interval, which is simply the ratio of the average earthquake slip in previous events to the long-term slip rate. Because the slip in the 1868 earthquake was essentially unknown, the Working Group on California Earthquake Probabilities [*Working Group on California Earthquake Probabilities (WGCEP),* 1990] assumed coseismic slip of 1.5 ± 0.5 m based on empirical relations between slip and rupture length and a rupture length of 30 to 40 km. Given a long-term slip rate of 9 ± 2 mm/yr, they estimated a recurrence interval of 167 ± 67 years. It is worth noting that most of the stated variance in the recurrence estimate results from uncertainty in the coseismic slip.

In this paper, we use triangulation data collected before and after the 1868 earthquake to estimate the rupture length and average slip in the earthquake. Triangulation surveys in the San Francisco Bay region were conducted in the 1850s and 1880s and again following the 1906 earthquake in 1907. In their historic study, *Hayford and Baldwin* [1908] computed displacements for the periods 1860-1880 and 1880-1907, attributing them to the 1868 and 1906 earthquakes, respectively. The displacements computed by *Hayford and Baldwin* [1908] are generally small near the Hayward fault but increase to ~ 3 m at Loma Prieta and ~ 2 m at Ross Mountain (Figure 1). An earlier analysis of the 1880-1907 displacements [*Segall and Lisowski,* 1990] indicates that Hayford and Baldwin's anomalous results for that event were due to assumptions and methods of computation, rather than to errors in the triangulation data. Unfortunately, Hayford and Baldwin's results for the 1868 earthquake depended on incompletely specified assumptions and are therefore probably not reproducible. They wrote

> The displacements of 1868 were computed on the assumption that the line Mount Tamalpais to Mount Diablo had a certain length and azimuth before 1868 and a certain length

> and azimuth after 1868; Mount Tamalpais being supposed to be in a new position, but Mount Diablo unmoved. The two positions for Mount Tamalpais were derived from certain computations, based in turn on assumptions that certain other stations remained unmoved in 1868, or practically so. [*Hayford and Baldwin*, 1908, p.140].

In their reanalysis of the 1906 displacements, *Segall and Lisowski* [1990] used only repeated angle measurements. As we show here, there is only a single angle that was measured both before and after the 1868 earthquake. It is therefore necessary to introduce methods that allow one to use all the available data, not only repeated measurements. Here we employ a projection operator that removes the dependence of the data on initial station coordinates, allowing for simple estimation of station displacements and fault slip. This approach should be applicable to the analysis of other geodetic data sets, especially those that were not collected for the purpose of studying crustal motions.

We also address the suggestion that deformation rates in the decades preceding the 1906 earthquake were anomalously high [*Thatcher*, 1975]. According to *Hayford and Baldwin*'s [1908] results, the Farallon islands displaced 1.4 m relative to Mount Diablo between 1860 and 1880 (Figure 1). This represents an average displacement rate of 70 mm/yr, more than twice the 30 mm/yr observed in the past 20 years [*Lisowski et al.*, 1991]. *Thatcher* [1975] also noted that the astronomic azimuth from Mount Diablo to Mount Tamalpais increased by 7.84 arc sec between 1859 and 1882, which corresponds to a fault-parallel displacement rate of 120 mm/yr. *Savage* [1978] suggested that the azimuth change was due either to measurement error or to the 1868 Hayward earthquake, rather than anomalous deep slip on the San Andreas fault. We address these issues here by simultaneously estimating the slip in the 1868 earthquake and secular strain accumulation in the San Francisco Bay region, both with and without the suspect astronomic azimuth observation. To our knowledge this is the first such analysis of these data as well as the first determination of slip in the 1868 earthquake and strain accumulation in the decades prior to the 1906 earthquake.

Data

The data used for this study are the horizontal angle observations from triangulation surveys conducted between 1853 and 1891. The horizontal angles were measured with a theodolite, which is simply a telescope mounted on a graduated circle. By sighting the instrument to one station and then to another, the observer determined the angle between the two stations by taking the difference between the two readings. We obtained the original field notes from these surveys from the National Archives in Washington, D.C., with cooperation from the National Geodetic Survey. A complete description of the data is given by *Yu* [1995] and is available from AGU as an electronic supplement[1] to this manuscript.

Pre-1868 Measurements: 1853-1860

Two surveys were conducted between 1853 and the 1868 Hayward earthquake (Table 1 and Figure 2). In the first, primary stations from Rocky Mound south to Gavilan were observed by R.D. Cutts in 1854 with a 30-inch Gambey theodolite. Cutts also made measurements at secondary stations in the southern part of San Francisco Bay with a 20-inch Gambey in 1853-1854, connecting the Pulgas Base with the primary network. In the second survey, stations north of Rocky Mound to station Sulphur Peak were surveyed by several observers from 1855 to 1860 with a 12-inch Gambey. Field procedures and the number of independent observations were different in the two surveys [*Yu*, 1995].

All pre-Hayward earthquake triangulation measurements used repeating theodolites. With a repeating instrument, one measurement of an angle is made by observing the angle a number of times advancing around the circle. The cumulative angle is then divided by the

[1]Supporting data are available on diskette or via Anonymous FTP from kosmos.agu.org, directory APEND (Username = anonymous, Password = guest). Diskette may be ordered from American Geophysical Union, 2000 Florida Avenue, N.W., Washington, DC 20009 or by phone at 800-966-2481; $ 15.00. Payment must accompany order.

Table 1. Preseismic Survey

Station	Date	Station	Date
Santa Ana	only sighted	Rocky Mound	1854
Black Mountain	1854	Ross Mountain	1859
Santa Cruz	1854	Sonoma Mountain	1858-1860
Diablo	only sighted	Tamalpais	1859
Farallon	only sighted	Tomales	1855-1858
Gavilan	1854	Guano Island	1853
Loma Prieta	1854	Pise Hill	1854
Masters Hill	1854	East Pulgas Base	1853
Murphy	1854	West Pulgas Base	1854
Pajaro Mouth	1854	Sulphur Peak	1859
Red Hill	1854	Point Reyes Hill	1859
Ridge	1854	Bodega	1860

Triangulation measurements were made from the listed stations on the given dates. "Only sighted" means that the station was sighted to but not occupied with a theodolite.

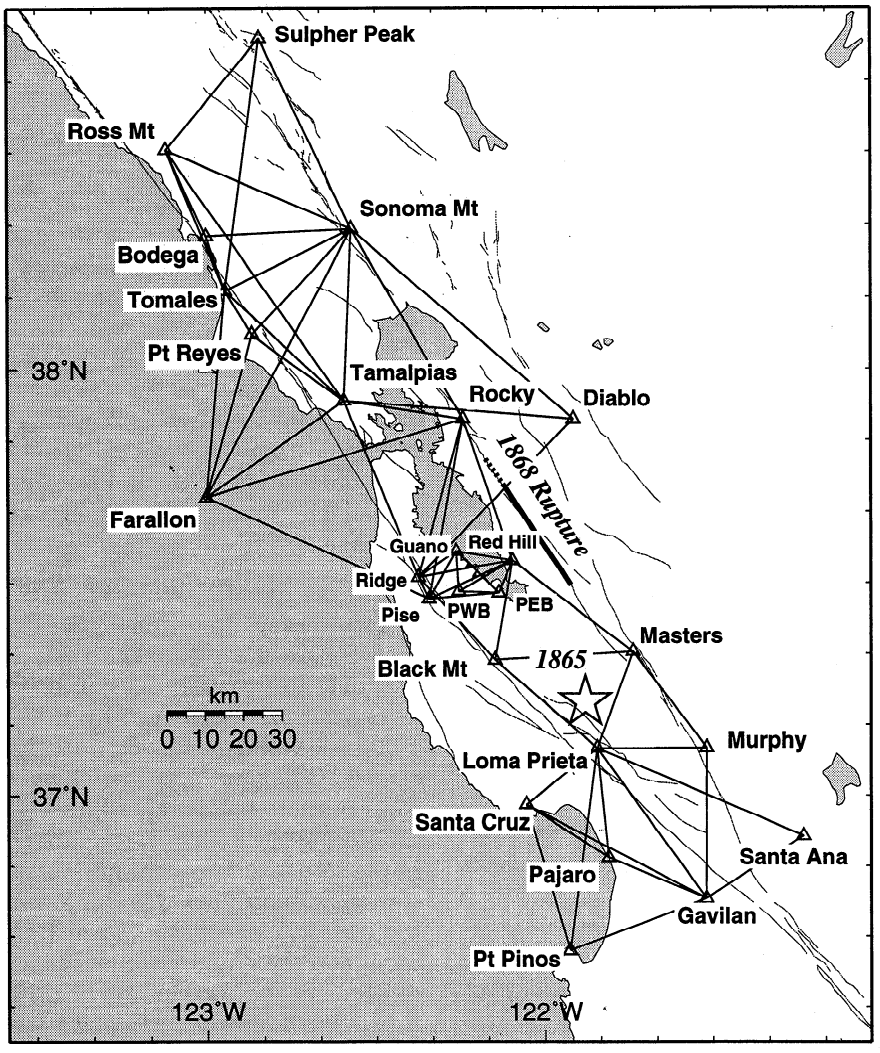

Figure 2. Pre-1868 survey, observed during 1853-1860 by the U.S. Coast Survey. The 1868 rupture is shown by the solid and dashed line. The approximate location of the 1865 earthquake is indicated by the star.

number of repetitions. This method prevents only one part of the circle being used. To eliminate systematic error from an eccentric vertical axis, the angle is re-measured in the same manner with the direction of the telescope reversed.

Field records show that the signal pole at station Ridge was "leaning and out of position" when observed from stations Rocky Mound and Red Hill. The notes go on to say that "Looking from Rocky Mound, the pole was too much to the left by 10 inches. Looking from Red Hill, the pole was too much to the right by 6 inches." We have excluded pointings to Ridge in our analysis, including ∠ Tamalpais - Rocky Mound - Ridge and ∠ Ridge - Rocky Mound - Red Hill. We do include the sum of the two angles ∠ Tamalpais - Rocky Mound - Red Hill, since this would not have been effected by the pointings to station Ridge, unless the pole tilted during the observations. In any event, our results do not change significantly if we exclude this angle or, for that matter, if we include all the observations to Ridge. The angle ∠ Tamalpais - Rocky Mound - Red Hill is the only angle repeated in the post-1868 triangulation survey, increasing by 11.04 arc sec between 1854 and 1885.

Post-1868 Measurements: 1876-1891

The post 1868 earthquake survey spans the interval 1876-1891 (Table 2 and Figure 3). With the exception of two stations, Rocky Mound and Red Hill, all measurements made after the earthquake used 20-inch-diameter direction theodolites. (Observations from Rocky Mound and Red Hill were made with a repeating theodolite.) With direction theodolites the observer picked an arbitrary zero mark and then measured angles from this mark. The observer would point at the first station, go onto the next station, and so forth, until all stations had been sighted. To eliminate errors from an unevenly graduated circle, the same set of stations was measured from different initial readings around the circle. These initial readings are called positions, and they

Table 2. Postseismic Survey

Station	Date	Station	Date
Santa Ana	1885	Mocho	1887
Diablo	1876, 1884	Sierra Morena	1883
Farallon	only sighted	Toro Mountain	1885
Loma Prieta	1884	Helena	1876, 1891
Red Hill	1885	Vaca	1880
Rocky Mound	1885	Monticello	1880
Tamalpais	1882		

Triangulation measurements were made from the listed stations on the given dates. "Only sighted" means that the station was sighted to but not occupied with a theodolite.

would be changed after a set of measurements had been made both direct and reversed at least once. Such a set is called a series. During this time period, it was standard U.S. Coast and Geodetic Survey practice for all primary station observations to have 23 positions with two series each, observational conditions permitting.

Error Analysis

There are several ways to judge the accuracy of triangulation measurements. One is to use triangle closure, the difference between the sum of the three angles in a given triangle and 180° plus the spherical excess. The spherical excess is given by $ma_1b_1\sin C_1$, where a_1 and b_1 are the lengths of two sides, C_1 is the included angle, and m is a factor which depends on the latitude. The rms closure in a network divided by $\sqrt{3}$ gives one estimate of the average observational error [*Bomford*, 1980].

Table 3 shows the closures for triangles in both networks. There are two triangles with significantly higher

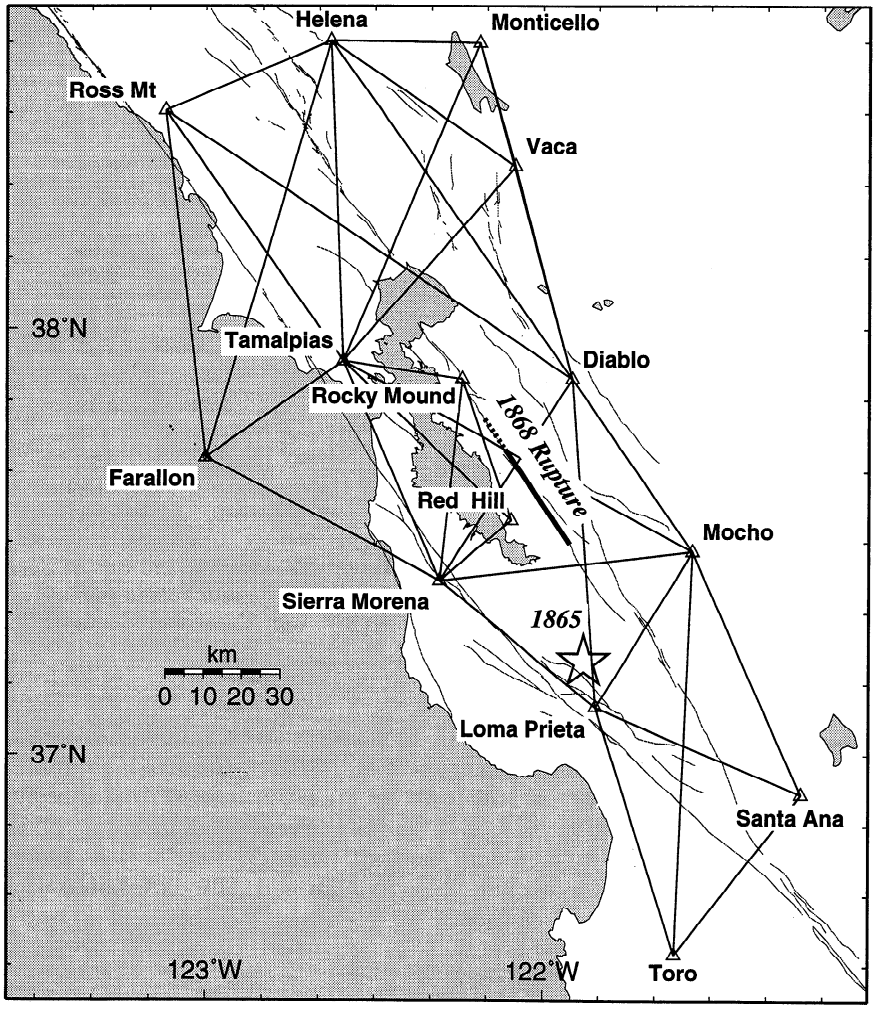

Figure 3. Post-1868 survey, observed during 1876-1891 by the U.S. Coast and Geodetic Survey. The 1868 rupture is shown by the solid and dashed line. The approximate location of the 1865 earthquake is indicated by the star.

Table 3. Closures of Pre-1868 and Post-1868 Triangulation

Triangle	Closure, arc sec
1853-1866 Closures	
Ross - Sulphur - Sonoma	-3.87
Ross - Sulphur - Tomales	3.29
Sonoma - Sulphur - Tomales	4.72
Ross - Bodega - Sonoma	0.73
Reyes - Tomales - Sonoma	0.63
Tamalpais - Reyes - Sonoma	-1.25
Tomales - Sonoma - Tamalpais	-4.89
Rocky - Tamalpais - Sonoma	-1.66
Bodega - Tomales - Sonoma	-0.81
Ross - Tomales - Sonoma	-3.78
Red Hill - Black - Ridge	-2.50 (-1.25*)
Red Hill - Ridge - Rocky Mound	4.53 (+2.05*)
Tamalpais - Ridge - Rocky Mound	4.77 (+6.00*)
Rocky - Red Hill - Pise	-0.80
Redhill - Black - Loma	-2.01
Black - Masters - Loma	-1.77
Murphy - Loma - Masters	-1.98
Gavilan - Loma - Murphy	-1.58
Gavilan - Pajaro - Loma	-2.72
Pajaro - Cruz - Loma	-2.77
Pise - Ridge - Guano	1.69
Pise - Guano - E. Pulgas	1.12
Guano - Red Hill - W. Pulgas	2.09
Guano - Red Hill - E. Pulgas	1.12
Guano - E. Pulgas - W. Pulgas	2.70
Red Hill - E. Pulgas - W. Pulgas	-0.31
1876-1891 Closures	
Tamalpais - Helena - Ross	0.75
Tamalpais - Vaca - Helena	-0.86
Vaca - Helena - Diablo	0.48
Helena - Vaca - Monticello	1.04
Ana - Toro - Loma	0.20
Ana - Loma - Mocho	0.24
Mocho - Loma - Toro	0.73
Toro - Mocho - Ana	0.26
Loma - Mocho - Morena	-1.48
Morena - Mocho - Diablo	0.48
Morena - Diablo - Loma	-1.37
Diablo - Mocho - Loma	0.37
Tamalpais - Red Hill - Rocky	-0.29
Red Hill - Rocky - Morena	-1.41

* Records show that signal pole at station Ridge was "leaning and out of position" when observed from stations Rocky Mound and Red Hill. The numbers in parenthesis are the triangle closures using corrections estimated by the U.S. Coast and Geodetic Survey.

closures in the area of interest, △ Tamalpais - Rocky Mound - Ridge and △ Red Hill - Rocky Mound - Ridge. These misclosures almost certainly result from the fact that the signal for Ridge was tilted when observed from Rocky Mound or Red Hill. For this reason, angles sighted to Ridge in these two triangles were excluded in our analysis. It is also notable that the misclosures are greater north of Tamalpais: angles that were measured in the 1855-1860 survey with the 12 inch Gambey theodolite. Because of this, we calculated standard deviations for the northern part of the network observed in 1855-1860 and the southern part of the network observed by Cutts in 1853-1854 separately.

An alternate method of estimating measurement error is based on the residuals from an unweighted network adjustment for station coordinates. This approach has the advantage of including all the data, not just observations in closed triangles. Assuming the observation errors are normally distributed with variance σ^2, then

$$\sigma^2 = \frac{\mathbf{r}^T\mathbf{r}}{N-p}. \quad (1)$$

Here $\mathbf{r}$ are the unweighted residuals, N is the number angles, and p is twice the number of stations minus the number of null vectors. In this case there are four null

Table 4. Error Analysis of Pre-1868 and Post-1868 Surveys

Survey Date	Method	σ, arc sec	Maximum Residual	Number of Stations	Number of Angles	Number of Closures
1853-1860	△ closure	1.42	3.77	24	94	23
(both surveys)	adjustment	1.75	3.05	24	94	...
1853-1854	△ closure	1.09	1.09	16	48	13
	adjustment	0.99	1.20	16	48	...
1855-1860	△ closure	1.75	3.06	10	41	10
	adjustment	1.97	2.72	10	41	...
1882-1887	△ closure	0.48	2.04	14	63	14
	adjustment	0.46	2.13	14	63	...

vectors corresponding to two horizontal translations, rotation about a vertical axis, and scale.

Table 4 shows the results of the error analysis for the various surveys. For each survey, σ was determined from triangle misclosure (row 1) and from a network adjustment (row 2). The column "Maximum Residual" contains the largest misfit in units of σ. It is clear from these results that the 1853-1854 survey was of significantly higher quality than the 1855-60 survey. To be conservative, the larger of the two variance estimates was used. We assign an error of 1.1 arc sec to the 1853-1854 angles and 2.0 arc sec to the 1855-1860 angles (Table 5). The post-1868 triangulation was of very high quality; we assign an error of 0.48 arc sec to the postearthquake angle determinations (Table 5). Because the raw postearthquake observations were directions, there is a correlation of minus one-half the variance between adjacent angles [e.g. *Prescott*, 1976].

Method

There are two general approaches to using triangulation data to determine station displacements, strain, or fault slip. One approach utilizes only repeated observations, relating these to the displacements of the geodetic stations [*Frank*, 1966; *Savage and Burford*, 1970; *Thatcher*, 1975; *Segall and Lisowski*, 1990]. With this approach one only needs to know approximate station coordinates, which is an advantage since it is the displacements not the coordinates that are of interest. A further advantage is that errors that are common to both surveys, or to the mathematical models, tend to cancel. Unfortunately, this approach does not work for the 1868 earthquake, for which we have only one repeated angle. Out of 30 stations in the area, only eight were observed in both preearthquake and postearthquake surveys. Most of the angles observed from these eight stations involved stations that were observed only in one survey.

Table 5. Summary of Survey Errors

Survey Date	σ, arc sec	χ^2	Maximum Residual
1853-1854	1.10		
1855-1860	2.00		
1876-1891	0.48		
Pre-1868	...	1.05	2.67
Post-1868	...	0.97	2.04

It is possible, however, to determine the relative motion of the eight common sites, two of which (Rocky Mound and Red Hill) are quite close to the Hayward fault. The second approach is to explicitly determine the coordinates of the stations at each epoch and to difference the coordinates to determine displacements. This allows one to use all of the available data. The disadvantage with this approach is that triangulation observations do not resolve rigid-body translations, rotations, or changes in scale of the network. Thus one must apply additional constraints, or assumptions, when determining coordinates, and this must be done carefully so as not to bias the displacements. *Bibby* [1982] introduced a method for simultaneously estimating station coordinates and strain between two surveys, and this approach has been widely used [e.g. *Bibby*, 1981; *Walcott*, 1984; *Snay*, 1986; *Drew and Snay*, 1989].

The approach taken here is to first estimate approximate coordinates of the stations using all preearthquake and postearthquake data. This is valid because the displacements between the two epochs are of the order of meters, and at this stage we only require station coordinates to be accurate at the $\sim$ 100-m level. We then linearize the relations between the observations and coordinates for the two epochs. At this point we recognize that the coordinates are nuisance parameters and eliminate the dependence on them through application of a projection operator. Following this "denuisancing" step, we are left with linear equations in stations displacements, from which it is straightforward to determine displacement, fault slip, and strain.

Estimation of Initial Coordinates

The horizontal angle between stations A, O, and B is a nonlinear function of the coordinates of the vertices

$$\theta_{AOB} = f(\lambda_A, \phi_A, \lambda_O, \phi_O, \lambda_B, \phi_B) \qquad (2)$$

where λ_J and ϕ_J are the geodetic longitude and latitude of station J, [e.g. *Drew and Snay*, 1989]. Expanding (2) in a Taylor series about a priori estimates of the coordinates $\mathbf{x}_J^0 \equiv (\lambda_J^0, \phi_J^0)$ and retaining terms to first order leads to

$$\theta_{\mathrm{AOB}}(\mathbf{x}) - \theta_{\mathrm{AOB}}(\mathbf{x}^0) = \frac{\partial f}{\partial \mathbf{x}} \mathbf{dx} + \epsilon \tag{3}$$

where $\mathbf{dx} = \mathbf{x} - \mathbf{x}^0$, and ϵ are measurement errors. Equation (3) can be written more compactly as

$$\mathbf{d\theta} = A\mathbf{dx} + \epsilon \tag{4}$$

where $\mathbf{d\theta} = \boldsymbol{\theta}(\mathbf{x}) - \boldsymbol{\theta}(\mathbf{x}^0)$ and $A_{ij} = \partial f_i(\mathbf{x})/\partial x_j$ are the functional derivatives of the ith angle with respect to jth station's longitude or latitude.

The solution of (4) is not unique; rotations, uniform dilatation, and rigid-body translations can occur without changing the observed angles. From amongst the infinite number of possible solutions, we seek the one with minimum norm, that is, the one that minimizes $\|\mathbf{dx}\|$. The minimum norm solution is conveniently found from the natural or Moore-Penrose inverse $A^\dagger$

$$\hat{\mathbf{dx}} = A^\dagger \mathbf{d\theta} = V_p \Lambda_p^{-1} U_p^T \cdot \mathbf{d\theta}, \tag{5}$$

where $A = U\Lambda V^T$ is the singular value decomposition of A and p is the number of nonzero singular values.

The solution (5) is used to obtain updated coordinates $\mathbf{x}$ and the procedure iterated until the coordinate corrections become small, $\|\mathbf{dx}\| \rightarrow \mathbf{0}$.

Estimation of Displacements

The results of the previous calculation are estimates of the station coordinates at the initial epoch, in this case the preearthquake period, which we denote $\mathbf{x}_1$. Note that $\mathbf{x}_1$ is not the best estimate of the station coordinates at t_1 because we have used both preearthquake and postearthquake data in their estimation. However, these coordinates should be sufficiently close to the true coordinates that we can linearize the observation equations and write

$$\mathbf{d\theta}_1 = A_1 \mathbf{dx}_1 + \epsilon_1 \tag{6}$$

$$\mathbf{d\theta}_2 = A_2 \mathbf{dx}_2 + \epsilon_2, \tag{7}$$

where A_1 represents the network geometry at time t_1 with coordinates $\mathbf{x}_1$ and A_2 represents the network geometry at t_2 with coordinates $\mathbf{x}_2$. We assume that the observation errors are normally distributed with zero mean and covariance Σ_1 and Σ_2; that is, $\epsilon_1 \sim N(O, \Sigma_1)$ and $\epsilon_2 \sim N(O, \Sigma_2)$.

Note that the coordinates at t_2 are equal to the coordinates at time t_1 plus the displacements between the two epochs, so that

$$\mathbf{dx}_2 = \mathbf{dx}_1 + \mathbf{u} + \epsilon_c, \tag{8}$$

where ϵ_c represent centering errors, which we take to be of the form $\epsilon_c \sim N(O, \sigma_c^2 I)$, σ_c being the standard deviation of the centering error. In the 1850s geodetic stations were often

> designated by an earthen cone or glass bottle buried under the surface of the ground and marked on top by a stone or post. Where the station is on a rock, a copper bolt or a hole filled with lead or sulphur, will be found to designate the exact spot. [*U.S. Coast and Geodetic Survey*, 1851, p.165].

On soil sites therefore we estimate that centering errors of as much as $\sigma_c = 0.1$ m may have resulted.

The full system of equations is now

$$\begin{bmatrix} \mathbf{d\theta}_1 \\ \mathbf{d\theta}_2 \end{bmatrix} = \begin{bmatrix} A_1 \\ A_2 \end{bmatrix} \mathbf{dx}_1 + \begin{bmatrix} 0 \\ A_2 \end{bmatrix} \mathbf{u} + \begin{bmatrix} \epsilon_1 \\ \epsilon_2 \end{bmatrix} \tag{9}$$

which for compactness we write as

$$\mathbf{d\theta}' = \Psi' \mathbf{dx} + \Omega' \mathbf{u} + \epsilon' \tag{10a}$$

$$\epsilon' \sim N(O, \Sigma) \tag{10b}$$

where

$$\Sigma = \begin{bmatrix} \Sigma_1 & 0 \\ 0 & \Sigma_2 + \sigma_c^2 A_2 A_2^T \end{bmatrix}. \tag{11}$$

Note that the effect of the centering errors is to increase the variance of the post earthquake survey.

The system of equations is normalized by premultiplying (10) by a weight matrix W given by the Cholesky factorization of the inverse covariance matrix $\Sigma^{-1} = W^T W$. The weighted equations, which we denote by dropping the primes in (10), have errors that are normally distributed with unit variance $\epsilon \sim N(0, I)$.

At this point one could simultaneously estimate coordinate corrections $\mathbf{dx}$ and displacements $\mathbf{u}$. However, as was pointed out previously, constraints on the null space components of $\mathbf{dx}$ and $\mathbf{u}$ would be required. Generalized inverses could be used; however, a minimum-norm inverse of (10) has the undesirable consequence of minimizing the norm of the sum $\|\mathbf{dx} + \mathbf{u}\|$, rather than the coordinate corrections and displacements separately.

We suggest that it is preferable to recognize that the coordinate corrections are, in fact, only "nuisance" parameters and of no interest in their own right. We can solve for the displacements $\mathbf{u}$ after first projecting out the dependence of (10) on $\mathbf{dx}$. Such projection techniques have been used to remove the dependence of seismic velocity inversions on hypocentral coordinates [*Pavlis and Booker*, 1980].

Let

$$Q \equiv I - \Psi \Psi^\dagger \tag{12}$$

where I is the $N \times N$ identity matrix and N is the number of data. Premultiplying (10) by Q leads to

$$Q\mathbf{d\theta} = Q\Omega \mathbf{u} + \epsilon \tag{13a}$$

$$\epsilon \sim N(0, Q) \tag{13b}$$

since

$$Q\Psi = (I - \Psi\Psi^{\dagger})\Psi = \mathbf{0}, \tag{14}$$

$AA^{\dagger}A = A$, being a property of generalized inverses.

What has been done, in effect, is to project out all components of the data that might be due to coordinate error. Only the remaining component is related to displacement. As equation (13) depends only on $\mathbf{u}$, any of a variety of approaches can now be used to invert for displacement. In particular, an inner coordinate or minimum-norm estimate, that is, the least squares estimate that minimizes $||\mathbf{u}||$, is simply

$$\hat{\mathbf{u}} = (Q\Omega)^{\dagger}Q\mathbf{d}\boldsymbol{\theta}. \tag{15}$$

As before, the generalized inverse is conveniently found from the singular value decomposition, $(Q\Omega) = U\Lambda V^T$. The variance-covariance matrix of the displacements is

$$\mathrm{Cov}(\hat{\mathbf{u}}) = (Q\Omega)^{\dagger}Q[(Q\Omega)^{\dagger}]^T. \tag{16}$$

As the projection operator Q is symmetric and idempotent, $QQ^T = Q$.

Alternatively, one can obtain a "model coordinate" solution [*Segall and Matthews*, 1988], here denoted $\hat{\mathbf{u}}_m$, by using a prior model $\mathbf{u}_{\mathrm{prior}}$ to constrain the null space components of the displacement field. The model coordinate solution minimizes $||\hat{\mathbf{u}}_m - \mathbf{u}_{\mathrm{prior}}||^2$ and is given by

$$\hat{\mathbf{u}}_m = \hat{\mathbf{u}} + V_0V_0^T\mathbf{u}_{\mathrm{prior}}. \tag{17}$$

where $\hat{\mathbf{u}}_m$ is given by (15) and V_0 are the columns of V which correspond to the zero singular values of Λ.

If desired, the coordinate corrections can be found by substituting (15) into (10) to obtain $\Psi\mathbf{dx} = [I - \Omega(Q\Omega)^{\dagger}Q]\mathbf{d}\boldsymbol{\theta}$.

Estimation of Fault Slip

We model the 1868 rupture on the Hayward fault as a displacement discontinuity in a homogeneous, linear elastic half-space. The surface displacements are linearly related to fault slip and can be evaluated in closed form for spatially uniform slip on a rectangular dislocation surface [e.g., *Okada*, 1985]. If s is fault slip then

$$\mathbf{u} = \mathbf{k} \cdot s \tag{18}$$

where $\mathbf{k}$ is, in general, a matrix. For the 1868 Hayward earthquake, in which we attempt only to estimate the magnitude of the spatially averaged strike slip, s is a scalar and $\mathbf{k}$ reduces to a vector. We must also account for interseismic deformation that occurred between the two triangulation surveys. Denoting the interseismic displacement rate as $\dot{\mathbf{u}}_s$, then (18) is modified to read

$$\mathbf{u} = \mathbf{k}s + \dot{\mathbf{u}}_s(t_2 - t_1) \tag{19}$$

where $t_2 - t_1$ is the time interval between the triangulation surveys. Inserting (19) into (10) yields

$$\mathbf{d}\boldsymbol{\theta}' - \Omega'\dot{\mathbf{u}}_s(t_2 - t_1) = \Psi'\mathbf{dx} + \Omega'ks + \boldsymbol{\epsilon}'. \tag{20}$$

The data covariance is now modified so that the lower right submatrix is

$$\Sigma_2 + [\sigma_c^2 + \sigma_{\mathrm{sec-rate}}^2(t_2 - t_1)^2]A_2A_2^T. \tag{21}$$

Then, as before, we weight the equations and apply the projection operator Q. The resulting equation is of the form

$$Ks = \mathbf{d} + \boldsymbol{\epsilon}, \tag{22}$$

where $K = Q\Omega\mathbf{k}$ and $\mathbf{d} = Q[\mathbf{d}\boldsymbol{\theta} - \Omega\dot{\mathbf{u}}_s(t_2 - t_1)]$ is the projected triangulation data corrected for interseismic deformation.

Equation (22) is now solved, using standard methods for fault slip. For example, the least squares estimate of s is simply

$$\hat{s} = (K^TK)^{-1}K^T\mathbf{d}, \tag{23}$$

and the variance of the slip is

$$\mathrm{var}(\hat{s}) = (K^TK)^{-1}. \tag{24}$$

Simulations

Simulations were conducted to test the approach and numerical codes. Two meters of slip were assumed to occur on a 40-km-long vertical fault that ruptured from the surface to 10-km depth. The network geometry was based on the actual preearthquake and postearthquake surveys. There were no repeated angles. Some stations in survey 1 were not occupied in survey 2, and vice versa. Initial station coordinates were created by adding random normal errors with standard deviation of 200 m to the true coordinates. Random errors with $\sigma = 1.0$ arc sec were added to the correct angles to simulate measurement error. For each synthetic data set, initial estimates of station coordinates were obtained using all of the data. The denuisancing procedure was then used to estimate fault slip. The mean fault slip estimates after 1000 realizations was 2.07 m with a standard deviation of 0.79 m.

Results

Initial estimates of the station coordinates were taken from *Duvall and Baldwin* [1910]. A nonlinear least squares adjustment using both preearthquake and postearthquake triangulation yielded updated coordinates. The maximum correction was 201 m at Farallon Lighthouse. In order to correct for 30 years of interseismic deformation, we use the dislocation model of *Bürgmann et al.* [1994], which was fit to 20 years of geodolite data collected by *Lisowski et al.* [1991]. The model was used to predict the average interseismic velocity at each of the triangulation stations. Note that the *Bürgmann et al.* [1994] model is used to interpolate between geodolite stations and thus for our purposes need not accurately represent the mechanics of faulting in the San Francisco Bay area. We estimate the average error in the slip rate to be ~20% of the signal. The

predicted secular displacements for the 30-year interval are shown in Figure 1.

The 1868 Hayward fault earthquake was modeled as having uniform slip from the surface to a depth of 10 km. The southeastern end of the rupture was located at Warm Springs (coordinates 37°29' 44.16" North, -121°55' 18.84" East). We examined the fit to the triangulation data for fault lengths ranging from 30 km (San Leandro) to 60 km (Berkeley). Figure 4a shows the estimated fault slip with one standard error bounds. Figure 4b shows the probability that a random χ^2 variable would exceed the observed weighted residual sum of squares $P(\chi^2 > \text{RSS})$. The maximum likelihood occurs for a rupture length of 52 km, which is considerably longer than the 41-km-long upper bound of *Lienkaemper and Borchardt* [1992]. The data are not strongly sensitive to rupture length, however. Including the astronomic azimuth data, all rupture lengths are rejectable at the 95% confidence level. Excluding the astronomic azimuth data improves the goodness of fit substantially, indicating that these observations are inconsistent with the triangulation data. According to this measure, the maximum likelihood estimate without astronomic azimuth data is barely acceptable at the 95% confidence level. A more complete analysis of variance is presented below.

The estimated slip ranges from 3.5 to 3.0 m for rupture lengths of 30 to 40 km. Slip decreases rapidly for rupture lengths greater than $\sim$ 50 km, as the northern end of the rupture passes the station at Rocky Mound (Figure 4a). The estimated slip at the maximum likelihood rupture length of 52 km is 1.9 ± 0.4 m. Given that small size of the data set and the presumed strong influence of observations involving either Rocky Mound or Red Hill on the estimated slip, there is reason to be concerned that the least squares estimation is dominated by a small number of outliers. This does not appear to be the case. The estimated fault slip is not influenced by whether or not we include the astronomic azimuth observations, nor is it appreciably altered by excluding suspect triangulation observations to station Ridge. As a further test, we estimated slip minimizing the L1 norm of the residuals. A numerical optimization approach was used to minimize $\|\mathbf{d}-\mathbf{K}s\|_1$, where $\mathbf{K}$ and $\mathbf{d}$ are the same as in (22). The L1 estimates agree quite well with those obtained by least squares (Figure 4a),

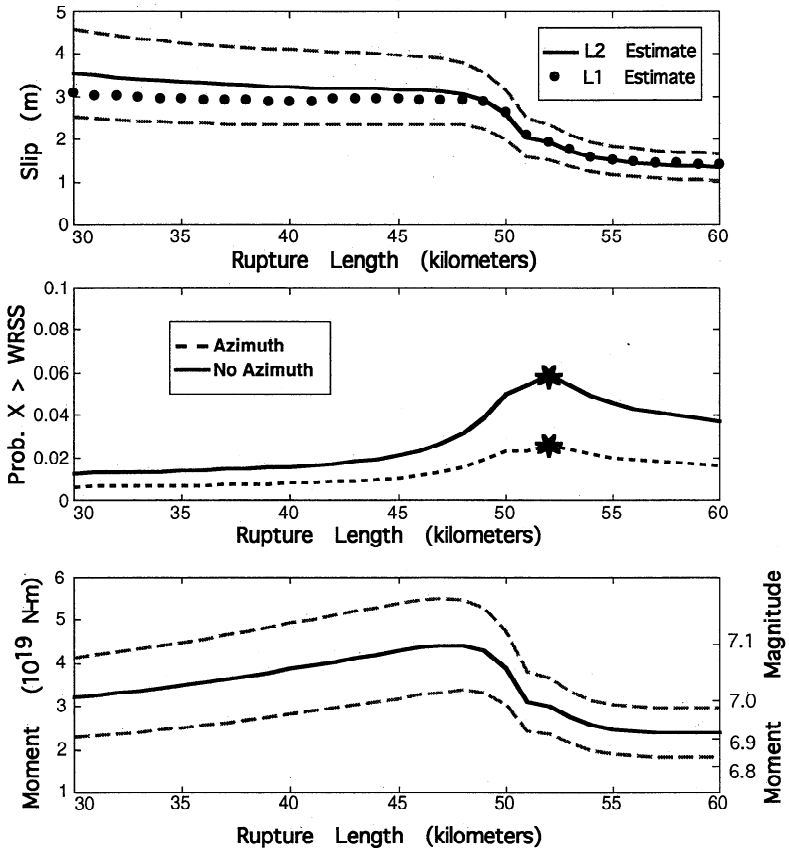

Figure 4. Results of fault slip estimation. (a) Average fault slip as a function of rupture length. Least squares (L2) estimates are shown (solid line) with $\pm 1\sigma$ error bounds (dashed lines). L1 estimates are indicated by solid circles. Slip estimates with and without the astronomic azimuth sightings are virtually identical. (b) Probability that a random χ^2 variable would exceed the observed residual sum of squares (RSS). Results are shown both including and excluding the astronomic azimuth sightings between Tamalpais and Diablo. (c) Estimated seismic moment (left scale) and moment magnitude M_w (right scale) as a function of rupture length with $\pm 1\sigma$ error bounds.

suggesting that the results are not dominated by a few outliers.

Because the slip decreases with increasing rupture length the seismic moment is relatively constant (Figure 4c). At the maximum likelihood rupture length of 52 km the seismic moment is $M_0 = 3.0\ (\pm 0.7) \times 10^{19}$ N m, assuming a shear modulus of 3.0×10^4 MPa, which corresponds to a moment magnitude of $M_w = 7.0$. For a 40 km rupture the slip is 3.2 ± 0.9 m, and the seismic moment is $M_0 = 3.9\ (\pm 1.1) \times 10^{19}$ N m, which also corresponds to $M_w = 7.0$. The data are not sensitive to the depth of rupture on the Hayward fault. In particular, a rupture depth of 15 km fits the data equally well. In this case the slip is slightly less, 1.7 ± 0.4 m for a 52-km-long rupture, and the moment is slightly greater, $M_0 = 4.1\ (\pm 0.9) \times 10^{19}$ N m. For the entire range of plausible rupture lengths and depths, M_w is essentially bounded between 6.9 and 7.1.

Displacements were computed for the eight stations that were observed in both preearthquake and postearthquake surveys, Santa Ana, Diablo, Farallon Lighthouse, Loma Prieta (Mount Bache in 1854), Red Hill, Rocky Mound, Ross Mountain, and Tamalpais (Table Mountain in 1854). A model coordinate solution excluding the astronomic azimuth observations is shown in Figure 5, where the a priori model is that computed from the best fitting coseismic model plus 30 years of secular motion. Recall that the a priori model is used only to constrain null-space components of the displacement field (that is, two rigid body translations, vertical axis rotation, and scale). Significant relative motion occurs between stations Rocky Mound and Red Hill, spanning the Hayward fault (Figure 5), which is not surprising given that the 1868 earthquake was the largest event to occur during this period.

Figure 6 shows the model coordinate solution including the astronomic azimuth observations. There is a pronounced increase in the magnitude of the displacements of Tamalpais, Farallon Light House, and Ross Mountain. Inclusion of the astronomic azimuths allows the vertical axis rotation to be estimated by the data, rather than being constrained by the a priori model. It

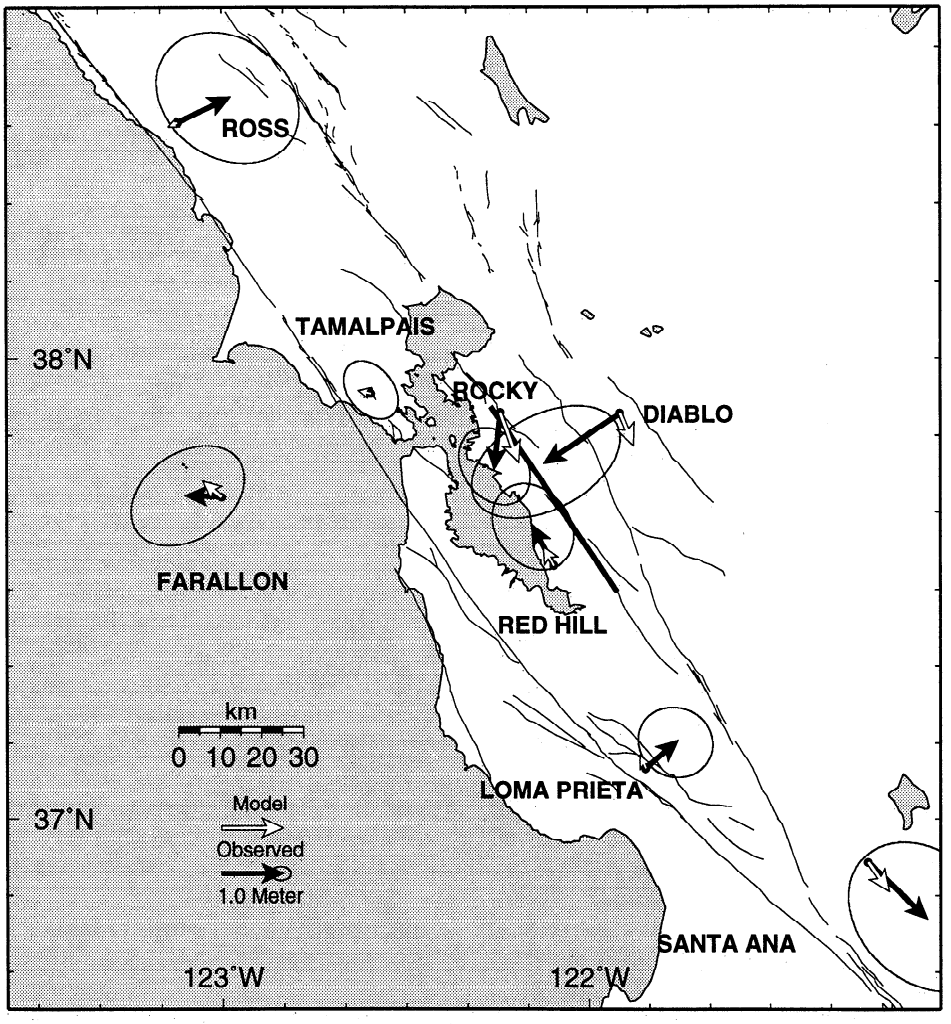

Figure 5. Calculated model coordinate displacements (solid arrows) using only triangulation observations. Confidence intervals are 95%. Rigid-body translation, rotation, and change in scale within the network are determined by an a priori model consisting of the best fitting coseismic rupture model plus 30 years of secular deformation (open arrows).

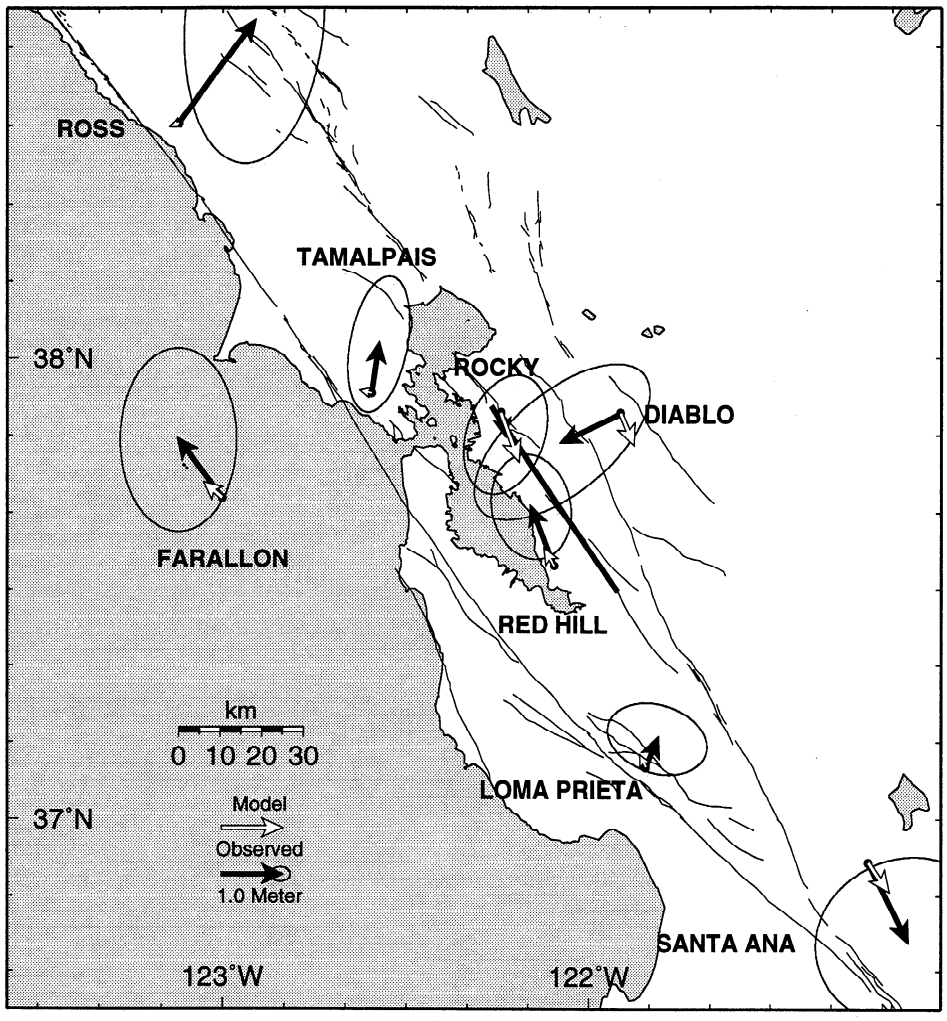

Figure 6. Calculated model coordinate displacements using triangulation data and astronomic azimuth observations between Tamalpais and Diablo (solid arrows). Confidence intervals are 95%. Rigid body translation and change in scale within the network are determined by an a priori model consisting of the best fitting coseismic rupture model plus 30 years of secular deformation (open arrows).

appears from these results that although the astronomic azimuth data do not influence the 1868 slip estimate, they do alter the displacement field. In fact, the displacements in the northern part of the network are similar to those computed by *Hayford and Baldwin* [1908] (Figure 1). Inclusion of the astro azimuth data presumably biased Hayford and Baldwin's displacements and any interpretations based on their results.

Figure 7 shows the displacements after subtraction of the expected secular displacement, relative to station Rocky Mound. Predicted displacements due to the best fitting coseismic model relative to Rocky Mound are shown for comparison. If our estimates of observational error are correct, we can be quite certain that Red Hill moved northwest relative to Rocky Mound. Stations Diablo, Loma Prieta, Tamalpais, and Ross all exhibit motion relative to Rocky Mound that is nominally significant at the 95% confidence level. As discussed below, the displacement of Loma Prieta may have been caused by the 1865 earthquake in the Santa Cruz mountains.

To examine the significance of the results, we test whether the data would be consistent with either no deformation, only secular deformation, or secular deformation plus 1868 coseismic deformation (Table 6). Without deformation, only coordinate corrections are estimated via the projection procedure. Including the astronomic azimuth observations, there are $N = 162$ observations, and $p = 57$ unknowns (2×30 stations minus three null vectors, corresponding to two rigid body translations and scale), so that $N - p = 105$. Excluding the astronomic azimuth observations, $N = 160$ and $p = 56$. The probability that a random χ^2 variable would equal or exceed the observed RSS is less than 0.1%. Including secular deformation does not change the number of degrees of freedom, since the secular model is not estimated from the data. The results in Table 6 indicate that there is less than a 1% probability that the data would have been generated solely by secular deformation of the magnitude observed today. According to these tests, we can confidently reject the

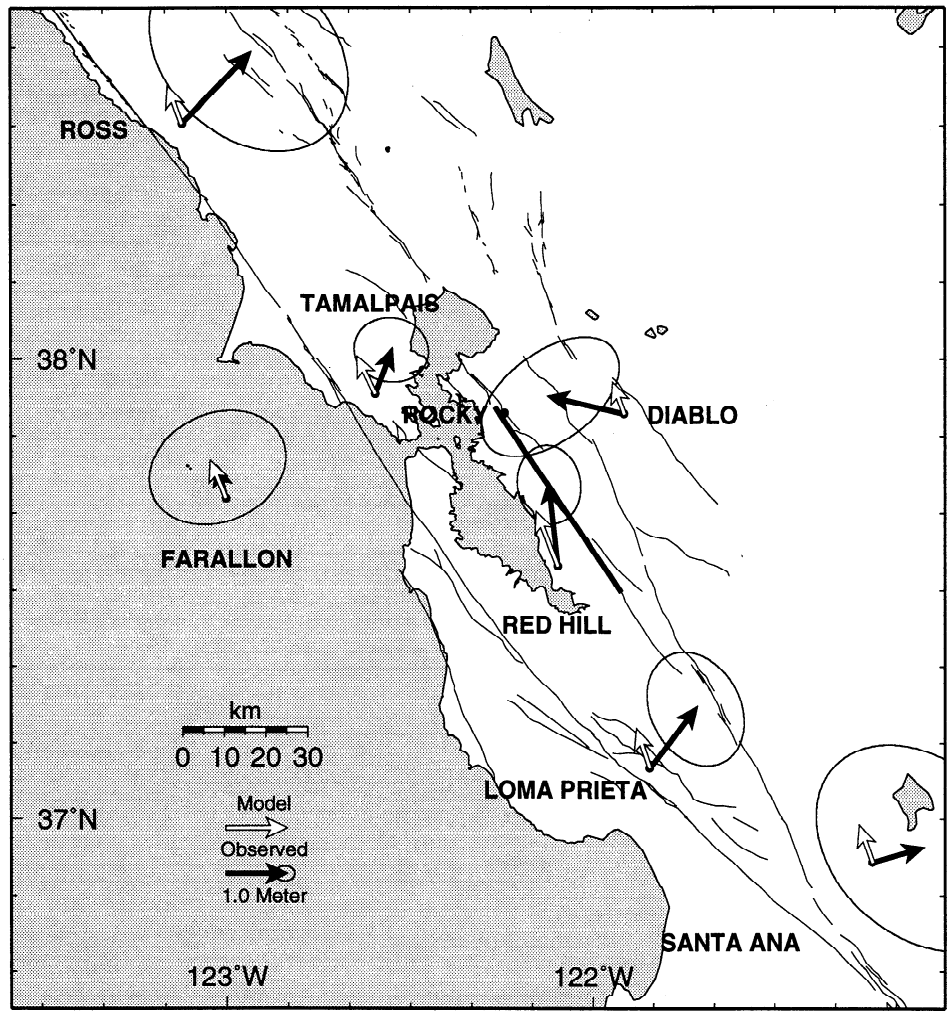

Figure 7. Calculated model coordinate displacements for the 1868 earthquake relative to Rocky Mound (solid arrows). Only triangulation observations are used. Confidence intervals are 95%. Rigid-body translation, rotation, and change in scale within the network are determined by an a priori model consisting of the best fitting coseismic rupture model plus 30 years of secular deformation (open arrows). Note that the relative displacement between Rocky and Red Hill is clearly significant at this confidence level.

null hypotheses that either no deformation, or only expected secular deformation, occurred between 1854 and 1885. On the other hand, there is between 3% and 6% probability that the data could have been caused by the modeled earthquake in addition to secular deformation, again depending on assumptions and the data used. Increasing the uncertainty in the secular model up to 33% of the signal does not significantly alter the numbers given here.

The final entry in Table 6 shows the misfit associated with arbitrary 1854-1885 displacements of the triangulation stations. For the displacement calculation, $p = 57 + 13 = 70$ ($13 = 2 \times 8$ stations for which we can compute displacement minus three null vectors), so that $N - p = 92$. The probability that a random χ^2 variable would equal or exceed the observed residual sum of squares per degree of freedom is 0.18. This component of the residual represents an irreducible error that no geophysical model can eliminate, since any model must predict a geometrically consistent displacement field. It is preferable to remove this "pure error" from the model residuals and test for model "lack of fit" [*Segall and Matthews*, 1988]. This is shown in Table 7 for two cases: secular deformation only and secular deformation plus 1868 coseismic deformation. The 92 degrees of freedom due to pure error (df_{PE}) is subtracted from the residual, resulting in 12 degrees of freedom for lack of fit (df_{LF}). We test for significant lack of fit taking the ratio

$$\rho \equiv \frac{\mathrm{SSLF}/df_{\mathrm{LF}}}{\mathrm{SSPE}/df_{\mathrm{PE}}}, \tag{25}$$

where SSLF and SSPE are the sum of squared residuals for lack of fit and pure error, respectively. If the model is correct, ρ should be distributed as an $F_{df_{\mathrm{LF}},df_{\mathrm{PE}}}$ random variable [*Segall and Matthews*, 1988]. Excluding coseis-

Table 6. Analysis of Variance Table

Model	N-p	$\frac{SS}{N-p}$	$P(\chi^2 \geq \frac{SS}{N-p})$
With Astronomic Azimuth Data: Centering Error $\sigma_c = 0.10$ m			
No displacement	105	1.64	< 0.001
Secular slip only	105	1.48	0.001
Secular slip + earthquake	104	1.29	0.026
Arbitrary displacement	92	1.13	0.177
With Astronomic Azimuth Data: Centering Error $\sigma_c = 0.05$ m			
No displacement	105	1.86	< 0.001
Secular slip only	105	1.62	< 0.001
Secular slip + earthquake	104	1.32	0.016
Arbitrary displacement	92	1.13	0.177
No Astronomic Azimuth Data: Centering Error $\sigma_c = 0.10$ m			
No displacement	104	1.57	< 0.001
Secular slip only	104	1.43	0.003
Secular slip + earthquake	103	1.23	0.059
Arbitrary displacement	92	1.13	0.177

mic deformation we find that $\rho = 3.70$. The probability of a random variable from an F distribution being this large or larger is only 0.06%, which strongly rejects the null model. Including the modeled 1868 earthquake, $\rho = 1.76$. A ratio this large or large would occur 6.7% of the time and is therefore not rejectable at the 95% confidence level. Nevertheless, the fit is not good, suggesting either the model of the 1868 earthquake is inaccurate or that there are other sources of deformation that have yet to be accounted for. We explore the latter possibility below.

A possible explanation for the poor fit could be that the secular model does not adequately describe the regional deformation during the latter part of the nineteenth century. An alternate possibility is that earthquakes other than the 1868 Hayward event contributed to the observed deformation. To test the former possibility, we forego the a priori secular model and instead estimate fault slip and two spatially averaged strain rates $\dot{\gamma}_1$ and $\dot{\gamma}_2$. According to convention, γ_1 represents right-lateral shear on N45°W trending planes, and γ_2 represents shear on E-W trending planes. We also estimate the rotation rate about a vertical axis $\dot{\omega}$; however, because the data set contains no information on scale, it is necessary to constrain the areal dilatation rate to zero. We thus replace (18) with $\mathbf{u} = \mathbf{k} \cdot s + \Gamma\dot{\gamma}$, where $\dot{\gamma}$ is a three vector containing the shear strain rate components and rotation rate and Γ is a matrix that relates shear strain to displacement [e.g., *Drew and Snay*, 1989]. This results in the following observation equation

$$Q\mathbf{d}\boldsymbol{\theta} = Q\Omega[\mathbf{k} \quad \Gamma] \begin{bmatrix} s \\ \dot{\gamma}_1 \\ \dot{\gamma}_2 \\ \dot{\omega} \end{bmatrix} + \boldsymbol{\epsilon}. \tag{26}$$

The covariance matrix includes the centering error; however there is no secular model applied and therefore no associated error.

Table 7. Pure Error and Lack of Fit

Source	*df*	SS	$\frac{SS}{df}$	ρ	$P(X \leq \rho)$
Secular Strain Only					
Model residual	104	148.8	1.43	...	...
Pure error	92	104.4	1.13	...	...
Lack of fit	12	44.4	3.70	3.26	0.0006
Secular Strain Plus 1868 Earthquake					
Model residual	103	126.4	1.23	...	...
Pure error	92	104.4	1.13	...	...
Lack of fit	11	22.0	2.00	1.76	0.067

Astronomic azimuth data are excluded. Centering error is $\sigma_c = 0.10$ m.

As indicated in Table 8, when estimated together with coseismic fault slip, the regional shear strain rates are not significant. The estimated fault slip is somewhat greater, 2.50 ± 0.45 m, as opposed to 1.9 ± 0.4 m assuming the a priori secular model, as the uniform strain approximation underestimates the motion of Rocky Mound due to shallow fault creep. This model fits the data no better, and in fact slightly worse, than by the applying the a priori secular model. If one were to ignore fault slip and estimate only uniform shear strain, then the estimated $\dot{\gamma}_1$ is barely significant 0.27 ± 0.13 μ strain/yr. The rotation rate is significant, due to the questionable astronomic azimuth measurements from Mount Diablo to Tamalpais. Excluding the astronomic observations and constraining the rotation rate to zero does not significantly alter the estimated strain rates. In sum, if we account for deformation associated with the 1868 Hayward earthquake, there is no evidence for regionally high shear strain rates in the period 1854-1885.

Discussion

The triangulation data clearly recorded crustal deformation between 1854 and 1885. Regardless of the statistical test employed, we can reject the null model of no deformation with a high degree of confidence. It is nearly as likely that the data record deformation in excess of the secular deformation observed in the San Francisco Bay area during the past several decades. The fact that the largest relative displacements span the Hayward fault (Figure 5) strongly suggests that the 1868 earthquake was recorded by these measurements. The relative motion between Rocky Mound and Red Hill is significant at the 95 % confidence level (Figure 7). Indeed, models of the deformation including rupture on the Hayward fault significantly improve the fit to the data (Table 7). While there is significant trade-off between rupture length and slip amplitude, the seismic moment of the earthquake is well resolved by the data. The moment magnitude M_w is between 6.9 and 7.1, and the plausible (one standard error) range of moments is from ~ 2.0 to ~ 5.5 in units of 10^{19} N m.

The goodness of fit to the triangulation data is maximized if the northern end of the rupture is in the vicinity of Rocky Mound, which is approximately 2 km east of the Hayward fault trace. The data thus favor a rupture length of ~ 52 km, which is considerably longer than some previous estimates. Modified Mercalli intensities of VIII-IX, which extend for ~ 50 km along the Hayward fault as far north as Berkeley [*Toppozada and Real*, 1981], are consistent with our inferred rupture length. Absence of clear evidence for surface faulting north of San Leandro [*Lawson*, 1908] could be simply due to lack of reporting or to slip at depth without surface expression.

It is also unlikely that the rupture length or slip is seriously biased by shallow fault creep, at least of the magnitude that has been observed this century. The a priori secular model includes the best existing estimates of creep-rate on the Hayward fault [*Lienkaemper et al.*, 1991] which range from 5 to 9 mm/yr. Even assuming the creep rates on the Hayward fault exceeded these estimates by 5 mm/yr in the nineteenth century, this would add only 15 cm of relative motion. This is far less than the 1.5 to 3.5 m of coseismic fault slip estimated from the triangulation data.

Both the geodetic and intensity data favor a 50- to 55-km rupture length, which implies that the average slip during the earthquake was ~ 2.0 m. According to the time-predictable model employed by the Working Group on California Earthquake Probabilities [*WGCEP*, 1990] this leads to a recurrence interval of 222 ± 66 years, slightly longer than obtained by the working group. On the other hand, if the rupture length was 40 km, as previously suggested, the recurrence interval would be substantially longer, 355 ± 127 years. Given that at the time of this writing, 127 years have elapsed since the most recent large Hayward fault earthquake and that earthquakes are not truly time predictable, it would be prudent for those in the vicinity of the fault to anticipate a comparable event at any time.

As discussed previously, large displacements of stations Tamalpais, Farallon, and Ross Mountain calculated by *Hayford and Baldwin* [1908], and the 7.84 arc sec astronomical azimuth increase between Diablo and Tamalpais between 1859 and 1882 led to the suggestion that there may have been accelerated straining in the 50 years prior to the 1906 San Francisco earthquake [*Thatcher*, 1975]. Our analysis does not indicate that accelerated strain took place during this period. In fact, when we account for the coseismic deformation in 1868, the estimated shear strain rate on N45°W planes is less than would have been anticipated. Only by ignoring the 1868 earthquake is the estimated fault-parallel shear strain rate even marginally significant.

In light of our analysis, it now seems likely that the change in astronomic azimuth between Diablo and Tamalpais was biased. *Hayford and Baldwin* [1908] found a 5.38 arc sec increase in the azimuth of this baseline analyzing the triangulation data, which they took as corroborating the astronomical sightings. However, their displacements were computed on the assumption that "certain other stations remained unmoved in 1868,

Table 8. Strain Estimates

Model	$\dot{\gamma}_1$, μstrain/yr	$\dot{\gamma}_2$, μstrain/yr	$\dot{\omega}$, μradians/yr	Slip, meters
Strain + 1868 Earthquake	-0.01 ± 0.14	-0.19 ± 0.16	2.37 ± 0.76	2.50 ± 0.45
Strain only	0.27 ± 0.13	-0.25 ± 0.16	2.17 ± 0.76	...

Astronomic azimuth data are included.

or practically so" [*Hayford and Baldwin*, 1908, p.140]. Being doubtful of the motion of Rocky Mound and Red Hill, they may have held these stations fixed. Therefore any movement of these stations due to the 1868 event would be expressed as displacement of Tamalpais and would cause an apparent change in azimuth between it and Diablo. In fact, the angle observed from Rocky Mound to Red Hill and Tamalpais increased by 11.04 arc sec between 1854 and 1885. With Rocky Mound and Red Hill fixed, this is consistent with a 1.7-m northward displacement of Tamalpais, which is very close to the 1.6-m displacement computed by Hayford and Baldwin. The same angle change could, however, be explained by a southwestward movement of Rocky Mound, which is much more plausible for right-lateral movement on the Hayward fault in 1868. In other words, the 5.38 arc sec azimuth increase from triangulation used to support the 7.84 arc sec increase from the astronomical observations disappears if we allow right-lateral movement on the Hayward fault. Furthermore, when the azimuth change is included in the analysis, it results in large apparent rotations of the network, as seen in Figure 6 and in Table 8.

Even the best fitting models including secular deformation and coseismic slip in 1868 provide only a marginally acceptable fit to the data. Calculations estimating spatially and temporally uniform shear strain in the region did not improve the fit. The most likely explanation is that we have not yet accounted for all of the known seismic events in the San Francisco Bay area that occurred between the two geodetic surveys. These include a M 6 1/4 in 1858 in the San Jose region, a M 6 and M 6 1/2 in the southern Santa Cruz Mountains in 1864 and 1865, respectively, a M 6 near Los Gatos in 1870, and another M 6 in the Santa Cruz mountains in 1884 [*Ellsworth*, 1990].

Little is known about the 1865 earthquake. Comparison of isoseismals with the 1989 Loma Prieta earthquake indicates that the 1865 earthquake was located northeast of the Loma Prieta earthquake, closer to San Jose, and that the 1865 source was probably shallower [*Tuttle and Sykes*, 1992]. *Tuttle and Sykes* [1992] suggested that the 1865 event may have ruptured a reverse fault in the Foothills thrust belt; a compressional zone which bounds the southern Santa Cruz mountains and the Santa Clara valley and includes the Sargent, Berrocal, and Shannon faults. The Shannon fault is known to have been active in the Quaternary [*McLaughlin*, 1990], and geodetic measurements of San Andreas normal contraction and uplift following the 1989 Loma Prieta earthquake have been interpreted to have been caused by post seismic slip on faults within the Foothills thrust belt [*Bürgmann et al.*, 1992; 1995].

Given the absence of reported surface rupture during the 1865 earthquake and the paucity of geodetic stations in the likely source region, it is not possible to uniquely determine the fault geometry and location of this earthquake. It is possible, however, to rule out certain possibilities. The northeast, fault-normal displacement of Loma Prieta is inconsistent with thrust or right-lateral thrust oblique slip on the 1989 rupture surface. Indeed, normal faulting would be required on the 1989 rupture surface to fit the observations. Nor is strike slip on a vertical San Andreas fault a likely cause of the fault normal displacement. The 1906 earthquake displaced Loma Prieta to the southeast, parallel to the trace of the San Andreas, which is consistent with shallow right-lateral slip on a vertical fault [*Segall and Lisowski*, 1990]. In contrast, in 1989 Loma Prieta was displaced southward, reflecting the oblique right-reverse mechanism of that earthquake.

On the other hand, the data are compatible with the 1865 earthquake having been located on a shallow thrust fault northeast of the San Andreas fault within the Foothills thrust belt. A possible, although by no means unique, model is illustrated in Figure 8. The source is a 30° southwest dipping thrust extending from 1- to 5-km depth. The moment of the 1865 earthquake, which is all that is really estimable from the data, is $2 \pm 1 \times 10^{19}$ N m, corresponding to $M_w = 6\ 3/4$. The moment is dependent on source depth and geometry. We have not attempted to determine rigorous bounds on the moment, although uncertainties are likely to be at least 1/4 of a magnitude unit. Inclusion of both the 1868 and 1865 earthquakes improves the fit to the triangulation data. For the model shown in Figure 8, the lack of fit to pure-error ratio would be exceeded 13% of the time due to random errors, which is a significant improvement in fit relative to models with only the 1868 rupture. Much of the remaining misfit is associated with the apparent motion of Mount Diablo; however, Diablo was only sighted to in 1854 so that its position in the preearthquake survey is not well determined. Allowing for local motion of station Diablo increases the probability that the lack of fit to pure-error ratio would be exceeded to 37%. This indicates that with the exception of local motion of Mount Diablo, the data are well fit by the dislocations representing the 1865 and 1868 earthquakes.

Conclusions

Triangulation measurements from 1853 to 1891 recorded significant crustal motions in the San Francisco Bay area. The large relative displacements between stations Rocky Mound and Red Hill, on opposite sides of the Hayward fault, argue strongly for these displacements being caused by the 1868 Hayward earthquake. The data may also contain evidence of motion due to the 1865 earthquake near Loma Prieta. The triangulation data provide the first reliable slip estimate for the 1868 earthquake. The triangulation measurements together with the distribution of felt intensities suggest that the 1868 earthquake ruptured 50 to 55 km of the Hayward fault from Warm Springs to Berkeley, considerably farther north than previously assumed. The estimated strike slip for a rupture of this length is 1.9 ± 0.4 m, and the seismic moment is $M_0 = 3.0(\pm 0.7) \times 10^{19}$ N m. While the seismic moment

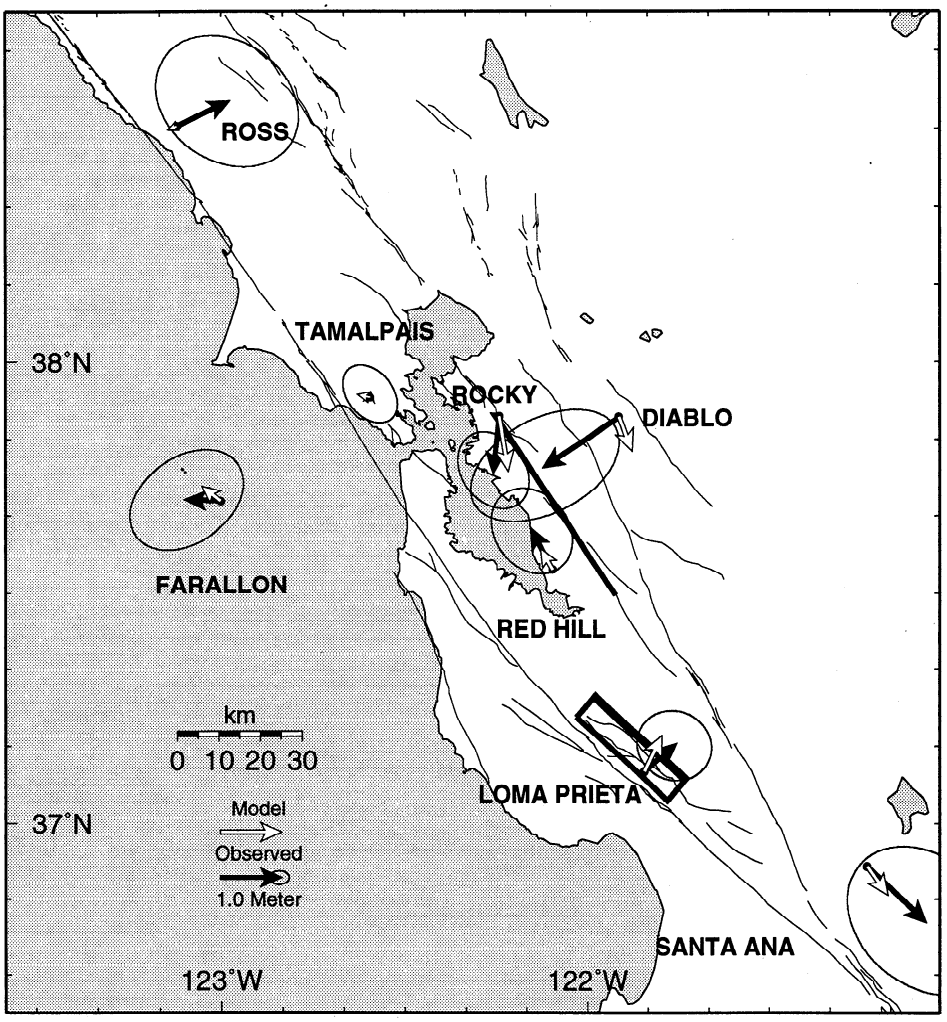

Figure 8. Comparison of observed displacements from Figure 5 (solid arrows) with a model including the coseismic displacements of the 1868 Hayward and 1865 Santa Cruz mountains earthquakes plus 30 years of interseismic deformation (open arrows).

is well resolved, i.e. all reasonable models have moment magnitudes M_w in the range of 6.9 to 7.1, the slip and rupture length are highly correlated. The corresponding time-predictable recurrence interval is $\sim 222 \pm 66$ years, comparable to, but slightly longer than, previous estimates. For shorter rupture lengths, the coseismic slip increases, and the corresponding time-predictable recurrence interval increases.

The northeastward directed displacement of the geodetic station on Loma Prieta likely resulted from the 1865 earthquake. The data are consistent with a $M_W \sim$ 6 3/4 thrust event northeast of the San Andreas fault in the southern Santa Cruz mountains thrust belt, a conclusion that is consistent with the distribution of felt intensities. The data are not compatible with reverse or right-reverse oblique slip on the 1989 Loma Prieta rupture surface, nor was the 1865 earthquake likely to have been a strike-slip event on the San Andreas fault.

Our analysis of the triangulation data does not support an earlier suggestion that regional strain rates in the San Francisco Bay area accelerated in the decades prior to the great 1906 earthquake. To the contrary, once the 1868 earthquake is accounted for, the data are quite consistent with the present-day pattern of interseismic deformation. The projection procedure employed here should prove useful in the analysis of other geodetic data sets, particularly those with few repeated observations.

Acknowledgments. We are extremely grateful to Richard Snay and Cindy Craig of the National Geodetic Survey, who were instrumental in obtaining the data for this study from the National Archives. We thank Wayne Thatcher, Mike Lisowski, Bill Ellsworth, and Roland Bürgmann for helpful discussions and Mark Murray, Shawn Larsen, Will Prescott, and Ken Hudnet for comments. This work was supported by U.S. Geological Survey grant 1434G2537 and the U.S. Geological Survey Graduate Intern program.

References

Bibby, H.M., Geodetically determined strain across the southern end of the Tonga-Kermadec-Hikurangi subduction zone, *Geophys. J. R. Astron. Soc., 66,* 513-533, 1981.

Bibby, H.M., Unbiased estimate of strain from triangulation data using the method of simultaneous reduction, *Tectonophysics, 82,* 161-174, 1982.

Bomford, G., 855 pp., *Geodesy*, Clarendon, Oxford, 1980.

Bürgmann, R., P. Segall, M. Lisowski, and J. L. Svarc, Rapid aseismic slip on the Berrocal fault zone following the Loma Prieta earthquake, *ES Trans. AGU, 73* (43), Fall Meet. Suppl., 119, 1992.

Bürgmann, R., R. Arrowsmith, T. Dumitru, and R. McLaughlin, Rise and fall of the southern Santa Cruz Mountains, California, from fission tracks, geomorphology, and geodesy, *J. Geophys. Res.*, 99, (B10), 20,181-20,202, 1994.

Bürgmann, R., P. Segall, M. Lisowski, and J. L. Svarc, Postseismic strain following the 1989 Loma Prieta earthquake from repeated GPS measurements, *U.S. Geol. Surv. Prof. Pap. 1550-D*, in *The Loma Prieta earthquake of October 17, 1989 - Postseismic effects, Aftershocks and Other Phenomena*, in press, 1995.

California Department of Conservation, Division of Mines and Geology, *Earthquake Planning Scenario for a Magnitude 7.5 Earthquake on the Hayward Fault in the San Francisco Bay Area*, 78 p., Sacramento, 1987.

Drew, A., and R.A. Snay, DYNAP: Software for estimating crustal deformation from geodetic data, *Tectonophysics, 162*, 331-343, 1989.

Duvall, C.R., and A.L. Baldwin, *Triangulation in California Part II,* Appendix 5, *Rep. U.S. Coast Geod. Surv., 1910,* 1910.

Ellsworth, W. L., Earthquake history, 1769-1989, in *The San Andreas Fault System, California*, edited by R.E. Wallace, *U.S. Geol. Surv. Prof. Pap. 1515*, 153-187, 1990.

Frank, F.C., Deduction of earth strains from survey data, *Bull. Seismol. Soc. Am.*, 56, 35-42, 1966.

Hayford, J. F., and A. L. Baldwin, Geodetic measurements of earth movements, in *The California earthquake of April 18, 1906, Report of the State Earthquake Investigation Commission*, vol. 1, edited by A. C. Lawson, pp. 114-115, Carnegie Inst. of Washington, Washington, D.C., 1908.

Lawson, A. C. (Ed.), *The California Earthquake of April 18, 1906, Report of the State Earthquake Investigation Commission*, vol. 1, Carnegie Inst. of Washington, Washington, D.C., 1908.

Lienkaemper, J.J., and G. Borchardt, Hayward fault: Large earthquakes versus surface creep, in *Proceedings of the Second Conference on Earthquake Hazards in the Eastern SF Bay Area, Spec. Pub.* 113, pp. 101-110, Calif. Dep. of Conserv., Div. of Mines and Geol., Sacramento, 1992.

Lienkaemper, J.J., G. Borchardt, and M. Lisowski, Historic creep rate and potential for seismic slip along the Hayward fault, California, *J. Geophys. Res., 96*(B11), 18,261-18,283, 1991.

Lisowski, M., J.C. Savage, and W.H. Prescott, The velocity field along the San Andreas fault in central and southern California, *J. Geophys. Res., 96*(B5), 8369-8388, 1991.

McLaughlin, R., Sargent fault zone at Loma Prieta, in *Field Guide to the Neotectonics of the San Andreas Fault System, Santa Cruz Mountains, in Light of the 1989 Loma Prieta Earthquake*, edited by D.P. Schwartz and D.J. Ponti, *U.S. Geol. Surv. Open File Rep., 90-274*, 19-22, 1990.

Okada, Y., Surface deformation due to shear and tensile faults in a half-space, *Bull. Seismol. Soc. Am., 75*, 1135–1154, 1985.

Pavlis, G.L., and J.R. Booker, The mixed discrete-continuous inverse problem: Application to the simultaneous determination of earthquake hypocenters and velocity structure, *J. Geophys. Res.*, 85(B9), 4801–4810, 1980.

Prescott, W.H., An extension of Frank's method for obtaining crustal shear strains from survey dat,a *Bull. Seismol. Soc. Am. 66*, 1847-1854, 1976.

Savage, J.C., Comment on "Strain accumulation and release mechanism of the 1906 earthquake," by W. Thatcher, *J. Geophys. Res. 83*(B11), 5487–5489, 1978.

Savage, J.C. and R.O. Burford, Accumulation of tectonic strain in California, *Bull. Seismol. Soc. Am., 60*, 1877-1896, 1970.

Segall, P., and M. Lisowski, Surface displacements in the 1906 San Francisco and 1989 Loma Prieta earthquakes, *Science, 250*, 1241–1244, 1990.

Segall, P., and M.V. Matthews, Displacement calculations from geodetic data and the testing of geophysical deformation models, *J. Geophys. Res.*, 93(B12), 14,954–14,966, 1988.

Snay, R., Horizontal deformation in New York and Connecticut: Examining contradictory results from the geodetic evidence, *J. Geophys. Res., 91*(B12), 12,695–12,702, 1986.

Thatcher, W., Strain accumulation and release mechanism of the 1906 earthquake, *J. Geophys. Res., 80*(35), 4862–4872, 1975.

Thatcher, W., Horizontal crustal deformation from historic geodetic measurements in southern California, *J. Geophys. Res., 84*(B5), pp. 2351-2370, 1979.

Thatcher, W., and M. Lisowski, Long-term seismic potential of the San Andreas fault southeast of San Francicso, California, *J. Geophys. Res., 92*(B6), 4771–4784, 1987.

Toppozada, T., C.R. Real, and D. L. Parke, *Preparation of isoseismal maps and summaries of reported effects for pre-1900 California earthquakes, U.S. Geol. Surv. Open File Rep., OF 81-0262*, 82 pp., 1981.

Toppozada, T., G. Borchardt, C. Hallstrom, and L. Youngs, Planning scenario for a major earthquake on the Hayward Fault, in *Proceedings of the Second Conference on Earthquake Hazards in the Eastern SF Bay Area, Spec. Publ. 113*, pp. 457-462, Calif. Dep. of Conserv., Div. of Mines and Geol., Sacramento, 1992.

Tuttle, M. P., and L.R. Sykes, Re-evaluation of several large historic earthquakes in the vicinity of the Loma Prieta and Peninsular segments of the San Andreas fault, California, *Bull. Seismol. Soc. Am., 82*, 1802-1820, 1992.

U. S. Coast and Geodetic Survey, *Report to Congress*, Washington, D.C., 1851.

Walcott, R. I., The kinematics of the plate boundary zone through New Zealand: A comparison of short and long-term deformations, *Geophys. J. R. Astron. Soc., 79*, 613-633, 1984.

Working Group on California Earthquake Probabilities, *Probabilities of large earthquakes occurring in the San Francisco Bay region, California, U.S. Geol. Surv. Circ., 1053*, 51 pp., 1990.

Yu, Ellen, Geodetic investigation of the Hayward earthquake of 1868, M.S. thesis, 106pp., Stanford Univ., Stanford, Calif., 1995.

P. Segall and E. Yu, Department of Geophysics, Stanford University, Stanford, CA 94305. (e-mail: segall@pangea.stanford.edu; ellen@pangea.stanford.edu)

(Received October 9, 1995; revised February 28, 1996; accepted March 6, 1996.)